20th IMEKO TC4 International Symposium and
18th International Workshop on ADC Modelling and Testing
Research on Electric and Electronic Measurement for the Economic Upturn
Benevento, Italy, September 15-17, 2014

The non-parametric amplitude estimation using MSL windows

Tomaž Lušin [1], Damir Ilić [2], Dušan Agrež [3]

[1] *Metrel d.d, Ljubljanska cesta 77, SI-1354 Horjul, Slovenia, e-mail: tomaz.lusin@siol.net*
[2] *University of Zagreb, Faculty of Electrical Engineering and Computing, Unska 3, 10000 Zagreb, Croatia, e-mail: Damir.Ilic@fer.hr*
[3] *University of Ljubljana, Faculty of Electrical Engineering, Tržaška 25, 1001 Ljubljana, Slovenia, e-mail: dusan.agrez@fe.uni-lj*

***Abstract* – The error reduction of the non-parametric amplitude estimation of the periodic signals with the three-point interpolated discrete Fourier transform (DFT) using cosine windows is presented. The paper analyzes and compares the systematic bias errors and the noise error behavior of the amplitude estimation changing the order of Rife-Vincent windows class I (RV1), which are designed for maximization of the window spectrum side-lobe fall-off, and minimum side-lobe level (MSL) windows, which are designed for minimization of the energy in the window spectrum main lobe. The lowest systematic bias errors can be found with the MSL windows and at the same time they better suppress the noise error contribution owed to smaller equivalent noise bandwidth (*ENBW*) than RV1 windows with the same order.**

***Keywords* – Amplitude, nonparametric estimation, DFT, Rife-Vincent windows class I, MSL windows**

I. INTRODUCTION

Estimations of the sinusoidal signal parameters are needed in many applications of measurement and instrumentation. Let us consider a discrete-time multi-frequency signal $g(t)$ acquired by sampling with frequency $f(\text{sampling}) = 1/t_s$, which is the base for estimations of signal parameters:

$$g(nt_s)_N = w(nt_s) \cdot \sum_{m=0}^{M} A_m \sin(2\pi f_m n t_s + \varphi_m) \qquad (1)$$

where f_m, A_m, and φ_m are frequency, amplitude, and phase of one component with index m among $M+1$, respectively. Index $n = 0, 1, \ldots, N-1$ is the current time index of the successive samples t_s apart.

In many cases the problem of evaluating the spectral performance of a given periodic signal reduces to the parameter estimation of each spectral component (frequency, amplitude, and phase). Estimation methods can be classified as parametric [1] and non-parametric [2],[3]. Parametric methods are model-based and have very good selectivity and statistical efficiency, but require computationally intensive algorithms and very good 'model agreement' with a real multi-component signal. For this reason, such methods are unsuitable for many estimation problems. The convergence of these multi-step procedures also much depends on the parameters' approximations of the first step. On the other hand, the model order issue does not apply when using nonparametric techniques, which estimate the spectral parameters of interest by evaluating first the DFT of the signal and then the parameters of the particular component. Using N samples of the signal (1), the DFT at the spectral line i is given by:

$$G(i) = -\frac{j}{2}\sum_{m=0}^{M} A_m \left[W(i-\theta_m) e^{j\varphi_m} - W(i+\theta_m) e^{-j\varphi_m} \right] \qquad (2)$$

where $W(*)$ is the spectrum of the used window $w(n)$, and $\theta_m = f_m/\Delta f = i_m + \delta_m$ is the signal component frequency divided by the frequency resolution $\Delta f = 1/(N\Delta t)$ where i_m is an integer value and the displacement term $-0.5 < \delta_m \le 0.5$ is caused by the non-coherent sampling. When failing to observe an integer number of periods of even a single tone, the tone energy is spread over the whole frequency axis, and the leakage from neighboring components can significantly bias estimations of the component parameters. The DFT coefficients surrounding one signal component are due to both the short-range leakage and the long-range leakage contributions from the second term of the investigated component, and from both terms of other components.

$$|G(i_m)| = \frac{A_m}{2}\left| W(\delta_m) e^{j\varphi_m} - W(2i_m + \delta_m) e^{-j\varphi_m} \right| + \sum_{k=0, k\neq m}^{M} |\Delta(i_k)| \qquad (3)$$

The long-range leakage contributions, which are the weak point of the non-parametric estimation approach, can be reduced in several ways: by increasing the measurement time, by using windows with a faster reduction of the side lobes (like the Rife-Vincent windows class I, etc. [4]), or by using the multi-point interpolated DFT algorithms [5]. It was shown that three-point DFT interpolation gives the optimum results [2]: it is symmetric arround the local peak amplitude DFT coefficient and equally suppress leakages comming from

ISBN-14: 978-92-990073-2-7

both sides (the third term in (3)); the minimal error curves are equal as with one-, five- and multi-point interpolations except the order of windows have to be changed when the Rife-Vincent windows are used.

In this paper we try to show the improvements of the systematic and the noise error reduction using the MSL windows in comparison to the RV1 windows. In estimations, the well-known expresion for the three-point estimations of amplitude (4) has been used [5]:

$$ {}_3A_m \doteq 2 \cdot \frac{\left[\left|G(i_m-1)\right| + 2\left|G(i_m)\right| + \left|G(i_m+1)\right|\right]}{\left|W(1+\delta_m)\right| + 2\left|W(\delta_m)\right| + \left|W(1-\delta_m)\right|} \qquad (4) $$

II. COSINE-SUM WINDOWS

Fixing the time of measurement, the reduction of the systematic leakage error mostly depends on the used window, which aim is to reduce the leakage energy in a trade-off the spectral resolution. Windows and their performances are bounded with two groups of windows defined by D.C. Rife and G.A. Vincent [6]: windows with the maximal side-lobe decay (MSD) are defined as RV1 windows and windows with the minimum side-lobe level are defined as Rife-Vincent windows class II (RV2). Both classes of windows are cosine-sum windows. Between them and their leakage performances are placed other windows like Rife-Vincent windows class III or Gaussian window, etc. [4]. In the paper, both boundary classes of cosine-sum windows are used to show their performance in the amplitude estimation. Classical windows RV1 are designed for maximization of the window spectrum side-lobes fall-off, based on the number of the time-domain window derivatives at the window ends, which are zero [7]:

$$ w(n) = \sum_{l=0}^{P} (-1)^l D_{\mathrm{RV1},l} \cdot \cos\left(l \frac{2\pi}{N} \cdot n \right) \qquad (5) $$

where $D_{\mathrm{RV1},l}$ are the weighted coefficients of cosines in the window function. A number of the used cosines functions defines window order P. The weighted coefficients can be calculated with $D_{\mathrm{RV1},0} = C_{2P}^{P} / 2^{2P}$ and $D_{\mathrm{RV1},l}(P) = C_{2P}^{P-l} / 2^{2P-1}$ ($l = 1, 2, ..., P$) using expression $C_x^y = x!/\left((x-y)!\,y!\right)$ [8]. RV1 windows are analytical well-known and the frequency spectrum can be expressed as (Fig. 1: curves a ($P = 1$) and c ($P = 4$)):

$$ W(\theta) = \frac{(2P)!}{2^{2P}} \cdot \frac{\sin(\pi\theta)}{\pi\theta} \cdot \frac{1}{\prod_{l=1}^{P}\left(l^2 - \theta^2\right)} \cdot \mathrm{e}^{-\mathrm{j}\frac{N-1}{N}\theta} \qquad (6) $$

and from here the denominator in (4) can be expressed and the amplitude can be generally estimated as [2]:

$$ {}_3A_m \doteq 2\left| \frac{2^{2P}}{(2P+2)!} \cdot \frac{\pi\delta_m}{\sin(\pi\delta_m)} \cdot \prod_{l=1}^{P+1}\left(l^2 - \delta_m^2\right) \right| \cdot \left(\left|G(i_m-1)\right| + 2\left|G(i_m)\right| + \left|G(i_m+1)\right| \right) \qquad (7) $$

Windows RV2 are designed for minimization of the window spectrum main-lobe width (the best resolution), for a given maximum level of the side-lobes relative magnitude [7]. Since their analytical manipulation is troublesome and need iterative procedure, more 'discrete' design windows as an approximation to RV2 windows are used in the measurement practice called minimum side-lobe level (MSL) cosine-sum windows [9]. Their window function is defined as in (5) with weighted coefficients $D_{\mathrm{MSL},l}$, which depend on the order P (Table 1). As with RV1 windows, MSL windows of order P have $P+1$ cosine terms in summation and $2(P+1)$ bins wide main-lobe width.

Table 1: Weighted coefficients of cosines for MSL windows $D_{\mathrm{MSL},l}$ ($l = 0, 1, ..., P$)

	$P=1$	$P=2$	$P=3$
$l=0$	0.5383553946707	0.4243800934609	0.3635819267708
$l=1$	0.4616446053293	0.4973406350967	0.4891774371450
$l=2$		0.0782792714423	0.1365995139787
$l=3$			0.01064112210553
	$P=4$	$P=5$	$P=6$
$l=0$	0.3232153788877	0.2935578950103	0.2712203605850
$l=1$	0.4714921439576	0.4519357723475	0.4334446123274
$l=2$	0.1755341299602	0.2014164714264	0.2180041228929
$l=3$	0.0284969901061	0.0479261092211	0.0657853432956
$l=4$	0.0012613570883	0.0050261964269	0.0107618673053
$l=5$		0.0001375555680	0.0007700127106
$l=6$			0.0000136808831
	$P=7$	$P=8$	$P=9$
$l=0$	0.2533176817029	0.2384331152778	0.22573453871301
$l=1$	0.4163269305810	0.4005545348644	0.38601229491509
$l=2$	0.2288396213720	0.2358242530472	0.24012942141061
$l=3$	0.0815750842593	0.0952791885838	0.10705423386646
$l=4$	0.0177359245035	0.0253739551662	0.03325916184017
$l=5$	0.0020967027490	0.0041524329075	0.00687337495232
$l=6$	0.0001067741302	0.0003685604163	0.00087516732380
$l=7$	0.0000012807021	0.0000138435559	0.00006008598933
$l=8$		0.0000001161808	0.00000171071647
$l=9$			0.00000001027272

Fig. 1 shows a trade-off between a fast side-lobe decay of RV1 windows and flatness of the side-lobe amplitudes of MSL windows, which reduce the energy in the main-lobe. In the vicinity of the mian lobe border (Fig. 1: arround $\theta \approx 2$ for order $P = 1$ and arround $\theta \approx 5$ for order $P = 4$) MSL windows perform lower spectrum values than RV1 windows and consequently lower bias errors in estimations if one adapt the order of window for specific value of θ. Energy reduction in the main-lobe also reduce the noise propagation defined by *ENBW* [4].

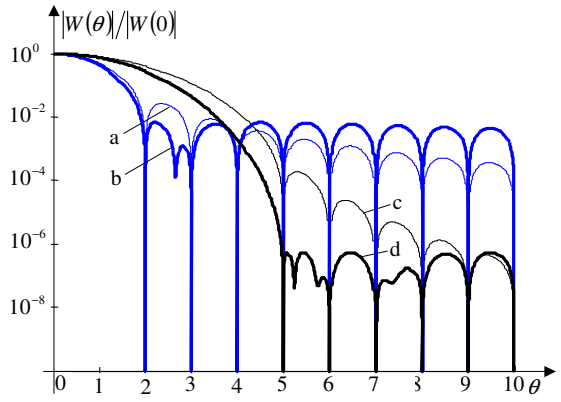

Fig. 1. The normalized spectra shapes of the RV1 windows (a and c) and the MSL windows (b and d); curves a and b - order $P=1$ and curves c and d - order $P=4$

MSL windows have better resolution than RV1 windows and lover bias error but the amplitude can't be express explicitely as with RV1 windows like in (7). The denominator $f\left(\left|W(\delta_m)\right|\right)$ in (4) has to be interpolated (Fig. 2.).

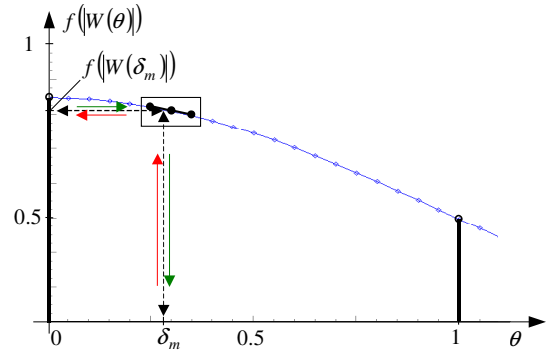

Fig. 2. Interpolation by zero-padding technique and then additional interpolation on the three local successive points around the investigated value $\delta_m \leftrightarrow f\left(\left|W(\delta_m)\right|\right)$

We use a two-step procedure to reduce the computational burden: first interpolation by a well-known zero-padding tecnique [10] to ideally increase resolution by factor 100 and then additional interpolation by the cubic polynomial on the three local successive DFT points around the investigated point (Fig. 2: points in the frame).

III. BIAS ERROR OF THE AMPLITUDE ESTIMATION

The effectiveness of the reduction of the leakage bias errors in the case of amplitude estimation are shown for the three-point IDFT estimations using MSL windows (Fig.3). The absolute relative errors $|e(A)| = |(A_{est.} - A)/A|$ of the amplitude estimation are checked for one sine component in the signal with a double scan, varying both frequency and phase because the long-range leakages are frequency- and phase-dependent ($A_m = 1$; $N = 1024$; $1 \le \theta \le 5.2$, $\Delta\theta = 0.01$ and $-\pi/2 \le \varphi \le \pi/2$, $\Delta\varphi = \pi/90$). The absolute maximum values of errors from 91 iterations at given relative frequency are compared for different orders $P = 1 \div 8$.

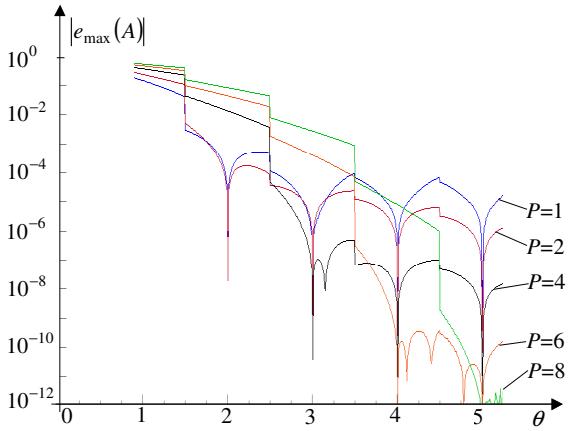

Fig. 3. Maximal errors of the amplitude estimation with the three-point interpolation of the DFT using MSL windows – frequency is known

Minimal curves of the maximal errors from Fig. 4 show that MSL windows have lower systematic bias errors in the amplitude estimation than RV1 windows, increasing the relative frequency θ and this is achieved with a slightly higher value of order P. The usage of MSL windows for amplitude estimation shows much lower bias error above relative frequency $2 < \theta$. If we have three and more signal cycles in the measurement interval ($3 < \theta$) or signal components are frequency interspaced for $6 < \Delta\theta$, the maximal bias errors drop to the level of 10^{-7} (for 140 dB).

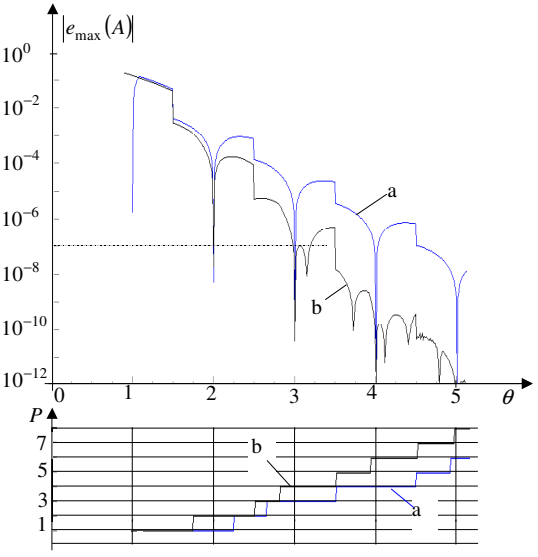

Fig. 4. Minimal curves of the maximal errors of the amplitude estimations with the three-point interpolation of the DFT using RV1 windows (a) and MSL windows (b) when frequency is known and the corresponding orders P=1…8 for the lowest maximal errors.

Since the MSL windows are designed for one of the shortest window spectrum main-lobe widths [9] one can conclude that the curve of the minimal error using three-point estimation and MSL windows (Fig.4: curve b) is very close to the minimal bias error for the non-parametric amplitude estimation in general.

In the expression of the amplitude estimation (4) is also the displacement term δ_m and estimation procedure is basically composed of two-steps: first the estimation of frequency by the known expresions for the three-point DFT interpolation (8) [2] and than amplitude estimation.

$$ {}_3\alpha_m = \frac{|G(i_m)|+|G(i_m-1)|}{|G(i_m)|+|G(i_m+1)|} \doteq \frac{|W(\delta_m)|+|W(1+\delta_m)|}{|W(\delta_m)|+|W(1-\delta_m)|} \quad (8a) $$

$$ \delta_m = f({}_3\alpha_m) \quad (8b) $$

Using RV1 windows the expression for displacement term is well-known (9) [2],[3] but for MSL windows the same interpolation procedure as in Fig. 2 need to be used in the reverse direction $\delta_m \leftarrow f({}_3\alpha_m) = f(|W(\delta_m)|)$.

$$ \begin{aligned} {}_3\delta_m &\doteq (P+1)\cdot\frac{1-{}_3\alpha_m}{1+{}_3\alpha_m} \doteq \\ &\doteq (P+1)\cdot\frac{|G(i_m+1)|-|G(i_m-1)|}{|G(i_m-1)|+2|G(i_m)|+|G(i_m+1)|} \end{aligned} \quad (9) $$

The two step procedure does't change much the error curves (Fig. 5) especially arround the intiger values of the relative frequency θ (a number of cycles in the measurement time) and this is mainly the case in the measurement practice. Fig. 6. shows the increased resolution around the intiger values by the testing condition with $\pm 10\,\%$ off-nominal frequency deviation $\theta/i_m = (i_m+\delta)/i_m = 1+\delta/i_m = 1\pm 0.1$. This condition was recommended in IEEE St. C37.118.1 [11] for phasor measurement units (PMU) and can also be used for amplitude estimation in dynamic measurements.

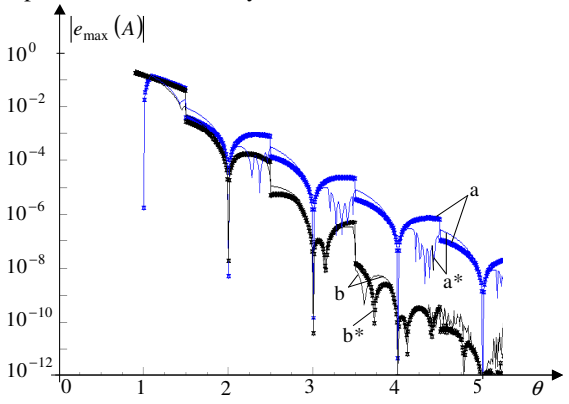

Fig. 5. Minimal curves of the maximal errors of the amplitude estimations with the three-point interpolations of the DFT using RV1 windows (a – frequency is known, a – frequency is estimated) and MSL windows (b – frequency is known, b* – frequency is estimated)*

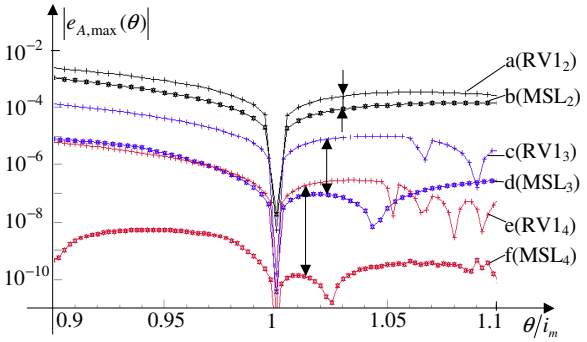

Fig. 6. Minimal curves of the maximal errors of the amplitude estimations with interpolations of the DFT using RV1 windows (curves a, c and e) and MSL windows (b, d and f) when two signal cycles are observed (a and b), when three signal cycles are observed (c and d), and when four signal cycles are observed (e and f). Waveforms are affected only by off-nominal frequency offset of $\pm 10\,\%$. In all cases frequency is estimated (8).

In the vicinity of $\theta = 2$, which means two signal cycles in the measurement interval, and with $\pm 10\,\%$ off-nominal frequency deviation ($i_m = 2 \rightarrow \delta = \pm 0.2$). (Fig 6: curves a and b), the best systematic bias behavior using RV1 windows is achieved with order $P = 1$, the Hann window (Fig 6: curve a), or MSL window order $P = 2$ (Fig 6: curve b). In the vicinity of $\theta = 3$ (Fig. 6: curves c and d, $i_m = 3 \rightarrow \delta = \pm 0.3$), very low maximal bias behavior is achieved using RV1 windows with order $P = 3$ (Fig 6c: around the level of 10^{-5}) or using better MSL windows and order $P = 3$ (Fig 7d: around the level of 10^{-7}). When fundamental signal component is dominant, the maximal bias errors drop on the level of 10^{-9} when using four signal cycles in the measurement interval and MSL window with order $P = 6$ (Fig. 4 and Fig. 6: curve f). This level of bias error is practically neglected against the noise error contribution.

IV. NOISE ERROR PROPAGATION

The reduction of the systematic error increases the contribution of the random noise part of the error [2]. To get an image how noise propagate through estimation algorithms using RV1 and MSL windows, in simulations, white noise with rectangular distribution, zero mean and the standard deviation $\sigma_t = A_{\text{noise}}/\sqrt{3}$ was added to signals in the time domain [12]. At every test point with changing frequency and phase, as in Fig 3, 50 trials of random added noise were used for the estimation of the amplitude standard deviation (Figs. 7 and 8: at every frequency altogether $37 \cdot 50 = 1850$ trials). The corresponding signal-to-noise ratio in the time domain was $SNR = A^2/(2\sigma^2)$. The noise propagations in the algorithms were compared with the Cramér-Rao lower bound [13],[14] (Figs. 7 and 8).

$$\sigma_{\mathrm{CRB}}(A) = A\frac{1}{\sqrt{N \cdot SNR}} \tag{8}$$

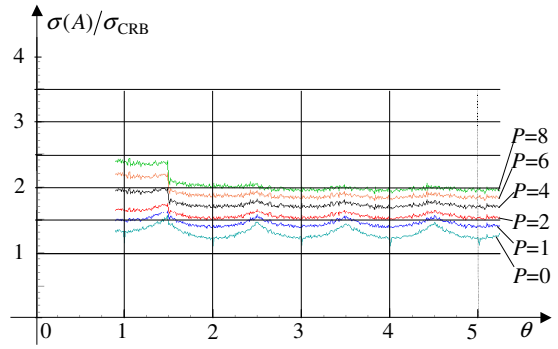

a) RV1 windows

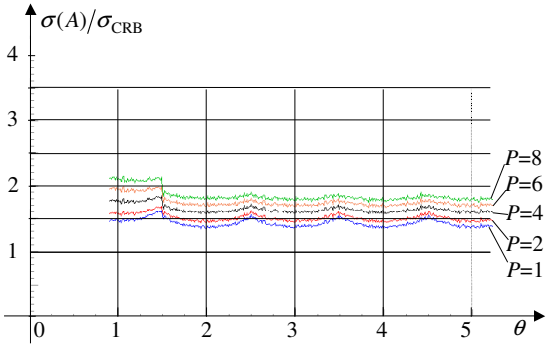

b) MSL windows

Fig. 7. Standard deviations of errors of the amplitude estimation in relation to the CRB – frequency is known; signal: $A=1$, $A_{\mathrm{noise}}=0.001$, $SNR=1{,}5\cdot10^{6}$ *(* $61{,}7\,\mathrm{dB}$ *);* $N=1024$; $\sigma_{\mathrm{CRB}}(A)=25.5\cdot10^{-6}$

The noise error contribution slightly increase in the two step estimation procedure $\delta_m \rightarrow A_m$ but basic shapes of error curves remain (Fig. 8).

Minimum side-lobe level windows perform very low systematic error and at the same time they also have a low noise error propagation because of the relatively small *ENBW* (Figs. 7b and 8b). In comparison with RV1 windows, they have lower levels of noise errors for the same value of order P (cf. Figs. 8a and 8b) and with an increase of order one can also noticed a smaller span of errors in relation to the CRB with the increase of order from $P=1$ to $P=8$.

V. EXPERIMENTAL RESULTS

To demonstrate the effectiveness of the proposed algorithms in reducing both estimation errors (phase depended bias error and noise contributions at different frequencies) we use digitizing voltmeter Agilent 3458A [15] for acquiring signal generated by a precise and stable voltage generator FLUKE 5700A [16] with the nominal sine voltage of $U_{\mathrm{n}}=7.00000\,\mathrm{V}$ and frequency $f_{\mathrm{n}}=50.00\,\mathrm{Hz}$.

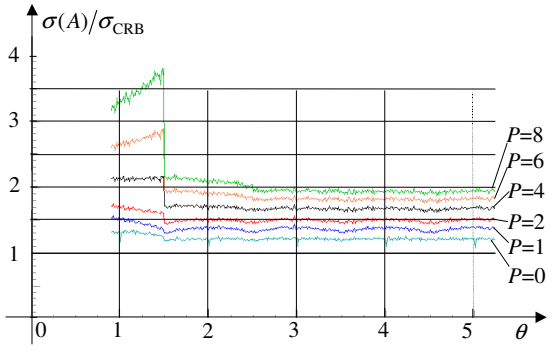

a) RV1 windows

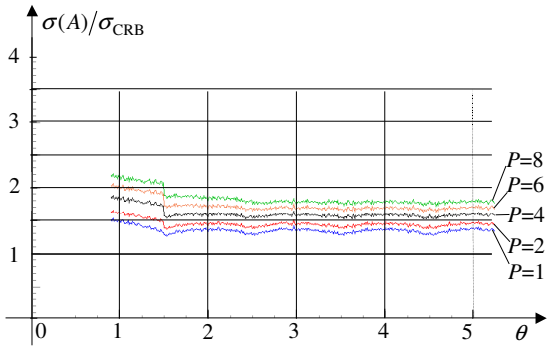

b) MSL windows

Fig. 8. Standard deviations of errors of the amplitude estimation in relation to the CRB – frequency is estimated signal: $A=1$, $A_{\mathrm{noise}}=0.001$, $SNR=1{,}5\cdot10^{6}$ *(* $61{,}7\,\mathrm{dB}$ *);* $N=1024$; $\sigma_{\mathrm{CRB}}(A)=25.5\cdot10^{-6}$

In both points of view of error propagation the MSL windows perform better results than RV1 windows in the amplitude estimation. This can be better seen if we combine both evaluated error contributions in the combined standard uncertainty (9) (Fig. 9). The standard uncertainty of type B evaluation [17] (or the effective value of the systematic bias contribution) is obtained by dividing the maximal error by the square root of two $w_{\mathrm{B}}(A)=e_{\max}(A)/\sqrt{2}$ because of the U-distribution of the probability density function. The systematic bias errors are phase-dependent with a sine-like shape when the signal phase is changed linearly and its *pdf* has a rectangular distribution. The standard uncertainty of type A evaluation is equal to the standard deviation of the added random noise $w_{\mathrm{A}}(A)=u_{\mathrm{A}}(A)/A=\sigma(A)/A$.

$$w_{\mathrm{c}}(A)=\sqrt{e^2_{\max}(A)/2+\sigma^2(A)/A^2} \tag{9}$$

In experiment, we change the sampling frequency by changing the timer time of voltmeter ($t_{\mathrm{timer}}=t_{\mathrm{s}}$, 'NRDGS 1024,TIMER'), while a number of the acquired samples remains constant $N=1024$. The aperture time of voltmeter was $t_{\mathrm{ap}}=10\,\mu\mathrm{s}$, what gives 18-bits of A/D converter resolution [15]. All results of the amplitude estimations were enlarged by the correction factor

$k_{\text{corr.}} = \pi t_{\text{ap}} f_{\text{n}} / \sin(\pi t_{\text{ap}} f_{\text{n}}) = 1.000000411$ owed to this aperture-integration time. To acquire signals from relative frequency $\theta = 1$ (one signal cycle in the measurement time) to $\theta = 5$, the timer time of voltmeter was changed from $t_{\text{s,min}} = 20\,\mu\text{s} \rightarrow \theta_{\text{min}} = f_{\text{n}} \cdot (N\, t_{\text{s,min}}) = 1.024$ by increment $\Delta t_{\text{s}} = 0.2\,\mu\text{s} \rightarrow \Delta\theta = f_{\text{n}} \cdot (N\, \Delta t_{\text{s}}) = 0.01024$ to maximal sampling time $t_{\text{s,max}} = 98\,\mu\text{s}$, what gives five acquired signa cycles $\rightarrow \theta_{\text{max}} = f_{\text{n}} \cdot (N\, t_{\text{s,max}}) = 5.0176$. At every frequency, the relative phase to signal zero-crossing point was changed uniformly between $-90\,\text{deg}$ and $90\,\text{deg}$ (minimum 85 points) and at every phase 30 trials was realized (altogether 2550 trials at every frequency).

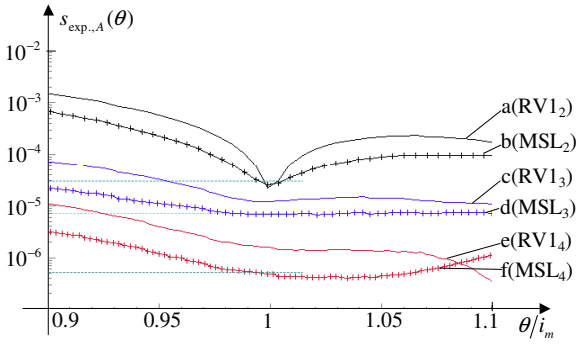

Fig. 9. Experimental standard deviations of the amplitude estimations with interpolations of the DFT using RV1 windows (curves a, c and e) and MSL windows (b, d and f) when two signal cycles are observed (a and b), when three signal cycles are observed (c and d), and when four signal cycles are observed (e and f). In all cases frequency is estimated.

For comparison to results in Fig. 6, we collect values of experimental standard deviations around the intiger values $i_m = 2, 3, 4$ by the testing condition with $\pm 10\,\%$ off-nominal frequency deviation $\theta / i_m = 1 + \delta / i_m = 1 \pm 0.1$ (Fig. 9). MSL windows allow lower bias errors to be attained. In the vicinity of $\theta = 2$ we reach the error level of $3 \cdot 10^{-5}$ with order $P = 2$ using MSL window. Near $\theta = 3$, the estimation error values of $6 \cdot 10^{-6}$ were achieved with order $P = 3$, and near $\theta = 4$, the error values of $5 \cdot 10^{-7}$ were achieved with order $P = 3$ using MSL window. We reach the error level of the calibrator uncertainty (FLUKE 5700A [16]: $w_{\text{c}}(A)_{7\text{V}} = 36 \cdot 10^{-6}$) already with two cycles in the measurement interval.

VI. CONCLUSIONS

The paper analyzes and compares the systematic bias errors behavior of the amplitude estimations using RV1 and MSL windows. The leakage effect can be effectively reduced by the three-point DFT interpolation, which equally suppress leakages comming from both sides on the frequency axis and performs the minimal error curves with changing the order of the used windows depending on the relative frequency θ. If we have three and more signal cycles in the measurement interval ($3 < \theta$) the maximal bias errors drop for $140\,\text{dB}$. At the same time MSL windows better suppress the noise error contribution owing to smaller *ENBW* than RV1 windows with the same order. The noise propagations using higher order of MSL widows are about 1.4- to 1.8-times larger than the CR lower bound.

REFERENCES

[1] G. D'Antona, A. Ferrero, Digital Signal Processing for Measurement Systems. Theory and Applications, Springer Science 2006.

[2] J. Štremfelj, D. Agrež, "Nonparametric estimation of power quantities in the frequency domain using Rife-Vincent windows", IEEE Trans. on Instrum. and Meas., vol. 62, no.8, August 2013, pp. 2171-2184.

[3] D. Belega, D. Petri, D. Dallet, "Frequency estimation of a sinusoidal signal via a three-point interpolated DFT method with image component interference rejection capability", Digital Signal Processing, vol. 24, no.1, January 2014, pp. 162-169.

[4] F. J. Harris, "On the use of windows for harmonic analysis with the discrete Fourier transform", Proceedings of the IEEE, vol. 66, no. 1, January 1978, pp. 51-83.

[5] D. Agrež, "Weighted Multi-Point Interpolated DFT to Improve Amplitude Estimation of Multi-Frequency Signal", IEEE Trans. Instrum. Meas. vol. 51, no. 2, April 2002, pp. 287-292.

[6] D. C. Rife, G. A. Vincent, "Use of the discrete Fourier transform in measurement of frequencies and levels of tones", Bell Syst. Tech. J. vol. 49, February 1976, pp. 197-228.

[7] G. Andria, M. Savino, A. Trotta, "Windows and interpolation algorithms to improve electrical measurement accuracy", IEEE Trans. Instrum. Meas. vol. 38, no. 8, August 1989, pp. 856-863.

[8] D. Belega, D. Dallet, "Multifrequency signal analysis by interpolated DFT method with maximum sidelobe decay windows", Measurement, vol. 42, no. 3, April 2009, pp.420-426.

[9] H.H. Albrecht, "Tailoring of minimum sidelobe cosine-sum windows for high-resolution measurements", The Open Signal Process. J., vol. 3, 2010, pp. 20-29.

[10] P. Babu, P. Stoica, "Comments on 'Iterative estimation of sinusoidal signal parameters' ", IEEE Signal Process. Letters , vol. 17, no. 12, Dec. 2010, pp. 1022-1023.

[11] IEEE Standard for synchrophasor measurements for power systems, IEEE Std. C37.118.1-2011, Dec. 2010.

[12] A. B. Sripad, D. L. Snyder, "A necessary and sufficient condition for quantization errors to be uniform and white," *IEEE Trans. Acoust., Speech Signal Process.*, vol. ASSP-25, no. 5, October 1977., pp. 442–448.

[13] A. Moschitta, P. Carbone, "Cramer-Rao Lower Bound for Parametric Estimation of Quantized Sinewaves", IEEE Trans. Instrum. Meas., vol. 56, no. 3, June 2007, pp. 975-982.

[14] P. Händel, Parameter estimation employing a dual-channel sine-wave model under a Gaussian assumption, IEEE Trans. Instrum. Meas., vol. 57, no. 8, August 2008, pp. 1661-1669.

[15] *3458A Multimeter - User's Guide*, Edition 5, 1988-2012 Agilent Technologies.

[16] *5700/5720ASeries - Multi-Function Calibrator - Operators Manual,* Rev. 2, FLUKE Cororation, May 1996.

[17] *Evaluation of measurement data — Guide to the expression of uncertainty in measurement*, JCGM 100, September 2008.